Light emission from an ambipolar semiconducting polymer field effect transistor: Analysis of the device physics

James S. Swensen[a] and Jonathan Yuen
Materials Department, University of California, Santa Barbara, California 93106 and The Center for Polymers and Organic Solids, University of California, Santa Barbara, California 93106-5090

Dan Gargas and Steven K. Buratto
Department of Chemistry and Biochemistry, University of California, Santa Barbara, California 93106 and The Center for Polymers and Organic Solids, University of California, Santa Barbara, California 93106-5090

Alan J. Heeger
Materials Department, University of California, Santa Barbara, California 93106; Department of Physics, University of California, Santa Barbara, California 93106; and The Center for Polymers and Organic Solids, University of California, Santa Barbara, California 93106-5090

(Received 30 April 2007; accepted 9 May 2007; published online 5 July 2007)

Light emitting field-effect transistors (LEFETs) were fabricated with a low work function metal (calcium) and a high work function metal (gold) as the source and drain electrodes. The gold electrode serves as the source for holes into the π band and the drain for electrons from the π^* band; the calcium electrode serves as the source for electrons into the π^* band and the drain for holes from the π band. For 65 V $< V_G <$ 103 V, the LEFET operates in the ambipolar regime. The emission zone has been spatially resolved (as it is moved across the channel by sweeping the gate voltage) using confocal microscopy; the full width at half maximum is 2 μm. At the gate voltage extremes (V_G=0 or V_G=150 V), the electron (hole) density extends all the way across the 16 μm channel such that the electron (hole) accumulation layer functions as the cathode (anode) for a light-emitting diode, with opposite carrier injection by tunneling; i.e., the carrier densities are sufficiently high that the accumulation layer functions as a low resistance contact, implying near metallic transport.
© *2007 American Institute of Physics*. [DOI: 10.1063/1.2752582]

I. INTRODUCTION

Ambipolar light emitting field-effect transistors (LEFETs) using luminescent semiconducting polymers were demonstrated recently by two independent research groups.[1–3] Here we present data obtained with calcium (Ca) and gold (Au) or silver (Ag) as the source and drain electrodes; the improved symmetry of the device performance enables a better understanding of the device physics. In addition, we make a direct comparison with the theoretical analysis of the device physics recently published by Smith and Ruden.[4]

The architecture of the LEFET is shown in Fig. 1. The structure is similar to that of conventional field-effect transistors (FETs), with a dielectric layer separating the gate from the semiconducting material. For the LEFET, we use a thin film of polypropylene-co-1-butene (PPcB) on silicon nitride (SiN_x) as the gate dielectric on heavily doped silicon wafer (n^{++}-Si), which functioned as the substrate and the gate electrode. The use of the PPcB overlayer minimizes the density of electron traps; the use of nonpolar polymers for the gate dielectric to enable electron transport was initially reported by Chua *et al.*[5] Ambipolar LEFETs are fabricated with two different metals for the top-contact source and drain electrodes (see Fig. 1): a low work function metal, Ca, and a high work function metal, Au or Ag [see the energy level diagram in Fig. 2(a)]. The high work function electrode serves as the source for holes into the π band and the drain for electrons from the π^* band, $[S_h(D_e)]$; the low work function electrode serves as the source for electrons into the π^* band and the drain for holes from the π band, $[S_e(D_h)]$.

As shown in Fig. 1, the LEFET can be viewed as a gate-induced *p-n* junction; light emission is expected, therefore, only in a narrow zone where the electron accumulation layer and the hole accumulation layer overlap. Detailed calculations of the width of the emission zone were recently published by Smith and Ruden.[4] The emission zone has been

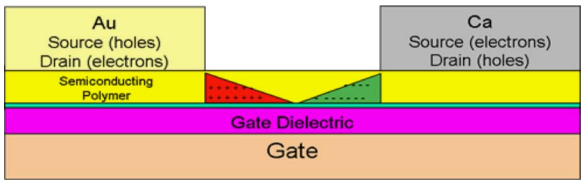

FIG. 1. (Color online) Schematic diagram of the device architecture of an ambipolar LEFET. The gold (Au) electrode serves as the source for holes into the π band and the drain for electrons from the π^* band; the calcium (Ca) electrode serves as the source for electrons into the π^* band and the drain for holes from the π. band. The thin green layer above the gate dielectric is the polypropylene-co-1-butene passivation layer. The red area shown in the channel represents the hole accumulation layer; the green area in the channel represents the electron accumulation layer.

[a]Electronic mail: jswensen@engineering.ucsb.edu

 © 2007 American Institute of Physics

Downloaded 20 Dec 2007 to 128.111.114.151. Redistribution subject to AIP license or copyright; see http://jap.aip.org/jap/copyright.jsp

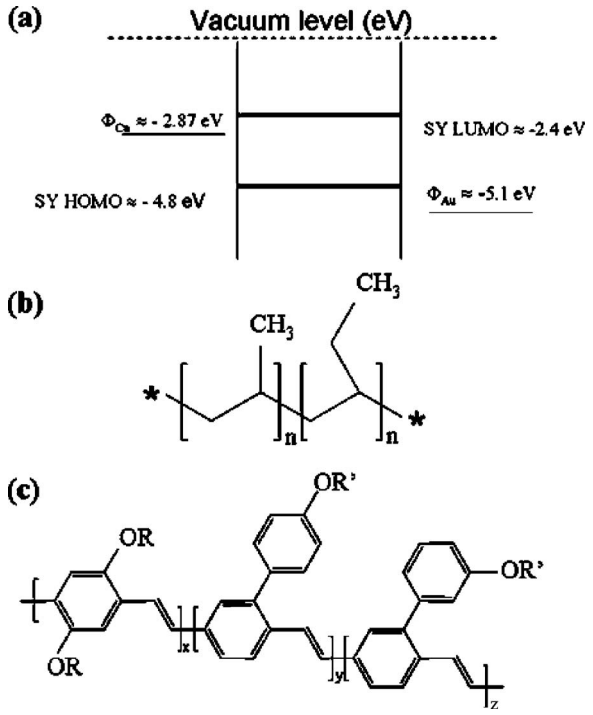

FIG. 2. (a) Energy level diagram showing the top of the π band (highest occupied molecular orbital) and the bottom of the π^* band (lowest unoccupied molecular orbital) of the luminescent semiconducting polymer, "SuperYellow." The Fermi energies of Ca and Au are shown. All energies are given with respect to the vacuum. (b) Molecular structure of polypropylene-co-1-butene (PPcB) which was used as the polymer passivation layer between the SiN_x gate dielectric and the semiconducting polymer. (c) Molecular structure of SuperYellow (SY), the soluble polyphylenvinylene (PPV) derivative used in this study as the semiconducting and light emitting polymer.

spatially resolved (as it is moved across the channel by sweeping the gate voltage) using confocal microscopy; the full width at half maximum is 2 μm.

At the gate voltage (V_G) extremes (V_G=0 or V_G =150 V), the electron (hole) density extends all the way across the 16 μm channel such that the electron (hole) accumulation layer functions as the cathode (anode) for a light emitting diode (LED), with opposite carrier injection by tunneling; i.e., the carrier densities are sufficiently high that the accumulation layer functions as a low resistance contact, implying near metallic transport.

II. EXPERIMENT

A heavily doped *n*-type silicon wafer functioned as both the substrate and the gate electrode. The n^{++}-Si gate electrode was coated with 400 nm of silicon nitride (SiN_x) deposited by plasma enhanced chemical vapor deposition. The SiN_x surface was cleaned by sonication in acetone followed by an isopropanol rinse and further sonication in isopropanol, then dried under a stream of nitrogen gas. The SiN_x was then passivated with a thin film of polypropylene-co-1-butene, 14 wt % 1-butene (PPcB) [see Fig. 2(b)].

20 mg of PPcB (obtained from Aldrich and used as received) were dissolved in 1 ml decaline at 190 °C. The substrate was placed on a Headway PWM32-PS-R790 Spinner, preset at 2500 rpm. PPcB solution (at 190 °C) was deposited

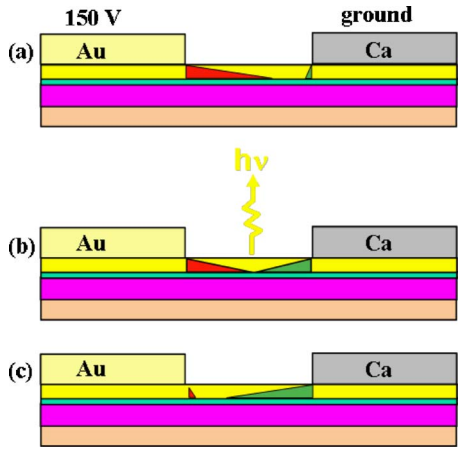

FIG. 3. (Color online) Schematic diagrams of the LEFET operation in the three important regimes: (a) $V_G < V_{SD}/2$; hole transport dominates. (b) $V_G \approx V_{SD}/2$; ambipolar transport dominates. (c) $V_G > V_{SD}/2$; electron transport dominates.

onto the substrate; as soon as it covered the entire surface, the spin coater was turned on for 60 s. The PPcB film was then dried on a hotplate in air at 200 °C for 1 min. Uniform, 100 nm films of PPcB were obtained (thickness determined by Dektak profilimetry). "SuperYellow" (SY), a soluble polyphylenvinylene (PPV) derivative obtained from Covion [see Fig. 2(c)], was then spin cast onto the substrate at 2500 rpm. After film deposition, the multilayer samples were annealed at 200 °C for 60 min. The calculated capacitance of the completed device was 9 nF/cm^2. The samples were then mounted onto a silicon shadow mask to complete the device fabrication by using the angled evaporation of Au followed by Ca. This fabrication process is described in detail in earlier publications.[1,6] The data reported here were obtained from LEFET devices with a 16 μm channel length and a 1500 μm channel width.

The LEFETs were tested using a Signatone probing station that is housed in a nitrogen glovebox. Oxygen count was ~1.5 ppm during device testing. A Keithley 4200 semiconductor characterization system was used to gather the electrical data; light emission was collected simultaneously with a Hamamatsu photomultiplier. For each run, the Ca electrode was always grounded and negative with respect to the Au (or Ag) electrode.

III. RESULTS AND DISCUSSION

The operation of the ambipolar LEFET is shown schematically in Figs. 3(a)–3(c). When a constant positive voltage of 150 V is applied between the Au and the Ca electrodes and the gate voltage is swept from 0 V to 150 V, the voltage drop between the gold $S_h(D_e)$ and the gate electrode decreases from 150 V at the beginning of the sweep to 0 V at the end of the sweep. Initially, an accumulation layer of holes is formed [Fig. 3(a)] at the interface between the semiconducting polymer and the PPcB dielectric layer extending toward the calcium $S_e(D_h)$ electrode. Hole current flows from the $S_h(D_e)$ electrode to the $S_e(D_h)$ electrode. As the gate voltage is swept toward 150 V, the voltage drop between the gate electrode and the $S_h(D_e)$ electrode decreases. As a re-

Downloaded 20 Dec 2007 to 128.111.114.151. Redistribution subject to AIP license or copyright; see http://jap.aip.org/jap/copyright.jsp

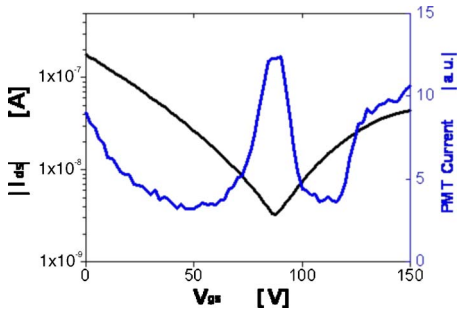

FIG. 4. (Color online) Black curve: total current between the Au and Ca electrodes as a function of the voltage applied at the gate electrode. Blue curve: light emission as detected by the photomultiplier.

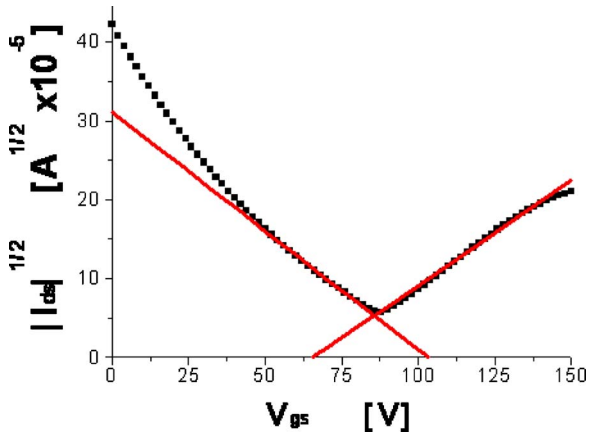

FIG. 5. (Color online) $|I_{ds}|^{1/2}$ plotted as a function of V_G, where I_{ds} is the total current between the Au and Ca electrodes.

sult, the hole accumulation layer reduces both in magnitude and in its extension across the channel, causing lower hole current at higher gate voltages [Figs. 3(b) and 3(c)]. Simultaneously, as the gate voltage is swept toward 150 V, the voltage drop between the gate electrode and the $S_e(D_h)$ electrode increases. As a result, the electron accumulation layer is formed and increases both in magnitude and in its extension across the channel, causing higher electron current at higher gate voltages [Figs. 3(b) and 3(c)].

Figure 4 shows the transfer data, channel current versus gate voltage and emitted light intensity versus gate voltage for an LEFET made with Au and Ca as the two electrode materials. The black curve represents the total current between the Au (the source for holes into the π band and the drain for electrons from the π^* band) and Ca (the source for electrons into the π^* band and the drain for holes from the π band) electrodes as a function of the voltage applied at the gate electrode. The blue curve shows the light emission intensity as detected by the photomultiplier. Note the near symmetry of both the channel current versus gate voltage and the emitted light intensity versus gate voltage (significantly better than observed with Ag as the high work function metal).[1] As implied by the energy level diagram in Fig. 2(a), Au would be expected to provide a nearly Ohmic contact to the superyellow polymer.

Maximum light emission intensity is expected when hole and electron currents are balanced, i.e., when each injected electron (hole) can radiatively recombine with a hole (electron). Because of the difference in hole and electron mobilities ($\mu_h > \mu_e$), this maximum occurs at approximately 90 V, rather than at 75 V (the midpoint in the range of the scan of the gate voltage in Fig. 4).

Note that at the voltage extremes, the emission intensity again increases. For example, at the beginning of the scan when the gate voltage equals 0 V, the device was emitting light. By imaging the channel with a microscope at 40× magnification, the emission zone was observed to be along the edge of the channel next to the calcium $S_e(D_h)$ electrode. We interpret this light emitted when the gate voltage equals 0 V as arising from more conventional emission from a polymer LED. A similar emission process has been discussed for hole only organic LEFETs,[7,8] and, in fact, it is likely the mechanism for light emission in all unipolar organic "LEFETs." As sketched in Fig. 3(a), the hole density extends all the way across the 16 μm channel length such that the hole accumulation layer functions as the anode for an LED with electron injection by tunneling from the Ca electrode. Similarly, as sketched in Fig. 3(c), when the gate voltage approaches −150 V with respect to the Ca electrode, the electron density extends all the way across the 16 μm channel length such that the electron accumulation layer functions as the cathode for an LED with hole injection by tunneling from the Au electrode. In other words, in these two limits the carrier densities (electrons in the π^* band or holes in the π band) are sufficiently high that the accumulation layer functions as a low resistance contact, implying near metallic transport.

In the saturation regime (where the source-drain voltage is larger than the gate voltage), the threshold voltages (V_{th}) can be determined from Eq. (1),

$$I_d = \mu C_i \frac{W}{2L}(V_g - V_{\text{th}})^2. \tag{1}$$

Thus, the threshold voltages for the onset of electron transport, V_{th}(electrons), and for the onset of hole transport, V_{th}(holes), are defined by plotting the square root of the drain current as a function of the gate voltage ($|I_{ds}|^{1/2}$ vs V_G) where I_{ds} is the total current between the Au and Ca electrodes and by extrapolating the electron dominated current and the hole dominated curves, respectively (see Fig. 5). The linear extrapolations yield the voltages for the turn-on of the hole current (103 V between the gate and the grounded Ca electrode) and for the turn-on of the electron current (65 V between the gate and the grounded Ca electrode). Thus, we find $|V_{\text{th}}(\text{electrons})| \approx 65$ V and $|V_{\text{th}}(\text{holes})| = 150 - 103$ V ≈ 47 V indicative of significant disorder with traps at the semiconductor-dielectric interface. For gate voltages in the range of 65 V $< V_G <$ 103 V, the device operates in the ambipolar regime with electrons in the π^* band and holes in the π band. The electron and hole mobilities can be obtained from the slopes of the two extrapolated lines in Fig. 5; $\mu_h = 2.1 \times 10^{-5}$ cm^2/V s and $\mu_e = 1.6 \times 10^{-5}$ cm^2/Vs.

Using their detailed theoretical analysis of the device physics, Smith and Ruden demonstrated excellent agreement between the measured and calculated total current between the $S_h(D_e)$ and the $S_e(D_h)$ electrodes (see Ref. 4).

Downloaded 20 Dec 2007 to 128.111.114.151. Redistribution subject to AIP license or copyright; see http://jap.aip.org/jap/copyright.jsp

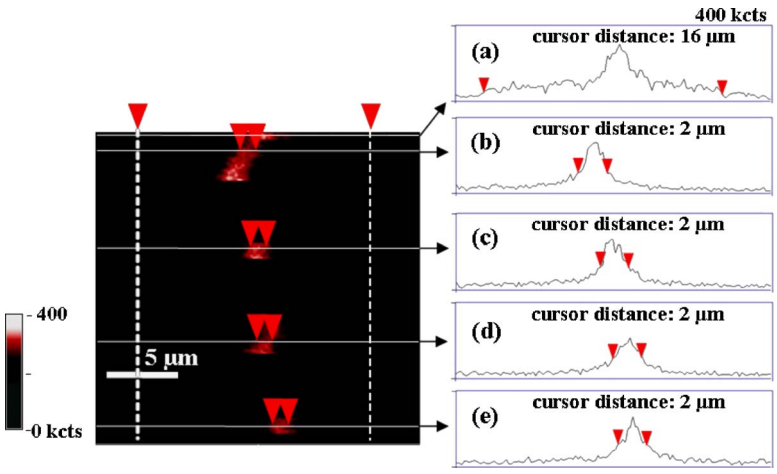

FIG. 6. (Color online) Confocal microscopy images of the emission zone collected as it moved across the channel region of the LEFET. Cross section plots of emission intensity vs lateral position in each scan are shown on the right. Cursors and the extended dotted lines depict the location of the electrode edges that define the channel region. Silver is the left electrode $[D_e(S_h)]$, and calcium is the right electrode $[S_e(D_h)]$. (a) V_d=115 V, V_s=−115 V, and V_g=0 V. (b) V_d=115 V, V_s=−111 V, and V_g=0 V. (c) V_d=115 V, V_s=−109 V, and V_g=0 V. (d) V_d=115 V, V_s=−105 V, and V_g=0 V.

As noted in the Introduction, the LEFET can be viewed schematically as a gate-induced *p-n* junction; light emission is expected only in a narrow zone where the electron accumulation layer and the hole accumulation layer overlap. Therefore, in the ambipolar regime, the location of the emission zone is controlled by the gate bias and moves across the channel (see Fig. 3 of Ref. 1). Smith and Ruden[4] calculated the gate-to-channel potential and the associated carrier densities (electrons and holes) as a function of distance within the channel, assuming (initially) an infinite recombination rate. Their calculations show that the gate-to-channel potential goes to zero in the gate-induced junction; i.e., where the hole and electron accumulation regions begin to overlap. This location, which moves as the voltage is scanned across the ambipolar region, defines the center of the light emission zone (and the center of the charge recombination zone). In the limit of infinite recombination rate, the recombination zone (and thus the emission zone) would be infinitely narrow. In reality, however, the width of the emission zone is determined by the recombination rate; the smaller the recombination rate, the wider the emission zone.

As demonstrated in Fig. 6, the emission zone has been spatially resolved using confocal microscopy. Confocal microscopy is a powerful imaging tool in which the highest possible resolution is achieved by collecting light at or near the diffraction limit ($\lambda/2$) and refocusing it in the confocal plane. The light collected from a sample is refocused in the confocal plane through a pinhole. Therefore, only light originating from the focal point is collected by the detector, whereas all light emanating from out-of-focus regions is rejected. Unlike conventional microscopy, the collected light forms a point source at the confocal plane and provides no spatial resolution. Spatial resolution is obtained by scanning the confocal spot over the sample, effectively creating an image point by point. Combining this scanning technique with incident laser excitation provides a high resolution, high sensitivity optical imaging system commonly referred to as laser scanning confocal microscopy (LCSM); details of the instrumentation used in the Buratto laboratory have been previously published.[9]

A portable sample chamber was made, which allowed for the encapsulation of the LEFET in an inert environment while interfacing it with the confocal microscope. Prior to device operation, the channel region was imaged with the confocal microscope. The channel region was defined by a region of high photoluminescence (PL) about 16 μm long with regions of no photoluminescence on both sides. The bright PL region corresponds to the luminescent semiconducting polymer in the channel. The dark regions on both sides of the channel are the silver and calcium electrodes; the metal electrodes block the laser from exciting the underlying luminescent polymer.

Once the confocal microscope was positioned over the channel, the laser illumination was turned off, and the LEFET was operated in the dark. Any electroluminescence within the channel was detected by the confocal microscope as it was scanned back and forth across the channel of the LEFET. The same collection principles described above for the LCSM experiment apply for the collection of electroluminescence from the LEFET. The only difference is the absence of laser excitation as the LEFET is electrically excited. Using this technique, high resolution images of the emission zone within the channel region of the LEFET were recorded.

The confocal microscopy data obtained from a LEFET are shown in Fig. 6 (the device structure was identical to that described in Ref. 1; i.e., n^{++} Si/SiN$_x$/PPcB/SY/Ca–Ag). Data were collected by rastering across the channel from left to right while slowly scanning from the bottom of the image and moving toward the top. A bias condition was set and held constant for a given period of time while the confocal microscope imaged the emission. Once a sufficiently long time had elapsed such that a good image was obtained, the bias was turned off, and the next bias was then set, applied, and held constant. The confocal microscope continued to scan in an upward direction while the biases were changed. For this reason, there is a dark region between the different images of the emission zone.

Each emission line corresponds to the bias conditions given in the figure caption. The tilt that can be seen in the longer collection times of the emission lines, the top image for example, shows a slow creep of the emission line toward the calcium electrode on the right side of the channel due to a bias induced threshold voltage shift for electron transport. Bias induced threshold voltage shift has been shown for hole transport semiconducting polymer FETs[10] and has been observed in our laboratory for electron transport as well.[11] An

Downloaded 20 Dec 2007 to 128.111.114.151. Redistribution subject to AIP license or copyright; see http://jap.aip.org/jap/copyright.jsp

analysis of the spatial intensity profile shows that the full width at half maximum of the emission zone is consistently 2 μm as it moves across the channel.

Smith and Ruden calculated a series of emission profiles assuming different recombination rates. For a recombination rate of 5×10^{16} s^{-1} cm^{-2} (the smallest value used in their simulations), they found a width of approximately 0.5 μm for the emission zone. Since the measured width is 2 μm, the actual recombination rate is somewhat slower than 5×10^{16} s^{-1} cm^{-2}; more precise evaluation of the recombination rate will require detailed numerical solutions of the equations developed by Smith and Ruden.

IV. CONCLUSION

In summary, the device physics of ambipolar light emitting field effect transistors was studied in detail. The threshold voltages for the onset of electron transport, V_{th}(electrons), and for the onset of hole transport, V_{th}(holes), were determined by extrapolating $|I_{ds}|^{1/2}$ vs V_G for electrons [current traveling from $S_e(D_h)\rightarrow S_h(D_e)$] and $|I_{ds}|^{1/2}$ vs V_G for holes [current traveling from $S_h(D_e)\rightarrow S_e(D_h)$]. We found that $|V_{\text{th}}(\text{electrons})|\approx65$ V and $|V_{\text{th}}(\text{holes})|\approx47$ V, indicative of significant disorder with traps at the semiconductor-dielectric interface. For gate voltages in the range of 65 V $<V_G<103$ V, the device operates in the ambipolar regime with electrons in the π^* band and holes in the π band. Recombination of electrons and holes takes place in a narrow zone of light emission within the channel. In the ambipolar regime, the location of the emission zone is controlled by the gate bias and moves across the channel as the gate voltage is swept between the threshold for electron transport and the threshold for hole transport. The emission zone was spatially resolved using confocal microscopy; the full width at half maximum is 2 μm. At the voltage extremes, for example, when the gate voltage approaches −150 V with respect to the $S_e(D_h)$ electrode (Ca), the electron density extends all the way across the 16 μm channel length such that the electron accumulation layer functions as the cathode for an LED with hole injection by tunneling from the Au electrode. Similarly, when the gate voltage approaches +150 V with respect to the $S_h(D_e)$ electrode (Au), the electron density extends all the way across the 16 μm channel length such that the hole accumulation layer functions as the anode for an LED with electron injection by tunneling from the Ca electrode. In other words, in these two limits the carrier densities (electrons in the π^* band or holes in the π band) are sufficiently high that the accumulation layer functions as a low resistance contact, implying near metallic transport. These very long distances for electron and hole accumulation, respectively, more than 10 000 repeated units on the semiconducting polymer chain and more than 10 000 interchain spacings imply the existence of well-defined π and π^* bands with a relatively low density of deep traps within the band gap. Since "SuperYellow" is relatively highly disordered when spin-cast from solution, we conclude that the well-defined band structure is a robust feature of semiconducting polymers.

The results presented here indicate that in the ambipolar regime, there is population inversion in the semiconducting polymer, with a high density of electrons in the π^* band ($>10^{19}$ cm^{-3} in the region near the interface between the semiconductor and the gate dielectric) and a high density of holes in the π band (again $>10^{19}$ cm^{-3} in the region near the interface between the semiconductor and the gate dielectric).[12] Thus, the LEFET provides a realistic route toward the fabrication of injection lasers from semiconducting polymers.

ACKNOWLEDGMENTS

Initial support for the LEFET work at UCSB was provided by the Air Force Office of Scientific Research (Charles Lee, Program Officer). Support for the research reported in this manuscript was obtained from the Division f Materials Research (Polymer Materials Program) within the National Science Foundation NSF-DMR-0602280. The confocal microscopy work was supported by the National Science Foundation (CHE-0316231). We thank Dr. Darryl Smith for initiating the detailed theoretical work required to properly describe the device physics and for communicating his results to us prior to publication.

[1] J. S. Swensen, C. Soci, and A. J. Heeger, Appl. Phys. Lett. **87**, 253511 (2005).
[2] J. Zaumseil, R. H. Friend, and H. Sirringhaus, Nat. Mater. **5**, 69 (2006).
[3] J. Zaumseil, C. L. Donley, J.-S. Kim, R. H. Friend, and H. Sirringhaus, Adv. Mater. (Weinheim, Ger.) **18**, 2708 (2006).
[4] D. L. Smith and P. P. Ruden, Appl. Phys. Lett. **89**, 233519 (2006).
[5] L.-L. Chua, J. Zaumseil, J.-F. Chang, E. C. W. Ou, P. K. H. Ho, H. Sirringhaus, and R. H. Friend, Nature (London) **434**, 194 (2005).
[6] J. S. Swensen, C. Soci, and A. J. Heeger, Proc. SPIE **6117**, 61170R–8 (2006).
[7] M. Ahles, A. Hepp, R. Schmechel, and H. von Seggern, Appl. Phys. Lett. **84**, 428 (2004).
[8] A. Hepp, H. Heil, W. Weise, M. Ahles, R. Schmechel, and H. von Seggern, Phys. Rev. Lett. **91**, 157406 (2003).
[9] K. D. Weston, P. J. Carson, H. Metiu, and S. K. Buratto, J. Chem. Phys. **109**, 7474 (1998).
[10] A. Salleo and R. A. Street, J. Appl. Phys. **94**, 471 (2003).
[11] J. S. Swensen, *Light Emission from an Ambipolar Semiconducting Polymer Field Effect Transistor* (University of California at Santa Barbara, Santa Barbara, CA, 2007).
[12] A. S. Dhoot, G. M. Wang, D. Moses, and A. J. Heeger, Phys. Rev. Lett. **96**, 246403 (2006).

Downloaded 20 Dec 2007 to 128.111.114.151. Redistribution subject to AIP license or copyright; see http://jap.aip.org/jap/copyright.jsp